Black Sea Journal of Engineering and Science
doi: 10.34248/bsengineering.1838054

Open Access Journal
e-ISSN: 2619 – 8991

Research Article
Volume 9 - Issue 2: 453-468 / March 2026

ENHANCEMENT OF OPTICAL CONVERSION EFFICIENCY IN SOLID-STATE LASER SYSTEMS THROUGH AN ADVANCED CAVITY DESIGN BY USING BOROSILICATE GLASS

Recep TORUN[1], Gülhan USTABAŞ KAYA[1]*

[1]*Zonguldak Bülent Ecevit University, Faculty of Engineering, Department of Electrical and Electronics Engineering, 67100, Zonguldak, Türkiye*

Abstract: The optical conversion efficiency (OCE) of a laser refers to the effectiveness of a laser system in converting electrical energy into usable laser radiation. Among the key parameters affecting this efficiency is the design of the optical cavity. This study examines the enhancement of optical conversion efficiency in a flash-lamp-pumped GentlelasePlus Alexandrite solid-state laser system through modification of the optical cavity structure. The original fused silica (quartz) cavity frame was replaced with a borosilicate (BK7) glass frame while maintaining the existing three-hole resonator configuration. The primary objectives are to improve efficiency and extend the operational lifetime of the laser system. Laser operation is evaluated at driving voltages of 900 Vdc and 1070 Vdc, and the resulting output energies are measured to calculate optical conversion efficiency (η_{OCE}). For an input energy of 1 J, the measured efficiencies were 0.1203 % for BK7 and 0.1378 % for quartz. At an input energy of 10 J, η_{OCE} values of 0.9407 % and 0.8935 % were obtained for BK7 and quartz, respectively. The results indicate that BK7 glass provides a 0.047 % higher efficiency compared to quartz and contributes to a 13 % overall improvement in system performance. Due to its lower material cost, ease of fabrication, and favorable optical performance, BK7 glass is proposed as a practical and cost-effective alternative to fused silica for optical cavity frames in Alexandrite laser systems.

Keywords: Alexandrite laser, Borosilicate glass, Flash-lamp-pumped, Optical conversion efficiency

***Corresponding author:** Zonguldak Bülent Ecevit University, Faculty of Engineering, Department of Electrical and Electronics Engineering, 67100, Zonguldak, Türkiye
E mail: gulhan.ustabas@beun.edu.tr (G. USTABAŞ KAYA)
Recep TORUN https://orcid.org/0000-0003-3897-8841
Gülhan USTABAŞ KAYA https://orcid.org/0000-0002-5643-0531

Received: December 10, 2025
Accepted: January 21, 2026
Published: March 15, 2026

Cite as: Torun, R., & Ustabaş Kaya, G. (2026). Enhancement of optical conversion efficiency in solid-state laser systems through an advanced cavity design by using borosilicate glass. *BSJ Engineering and Science*, *9*(2), 453-468.

1. Introduction

The fundamental principle of lasers which are used as light sources was first introduced by Einstein (1967). He emphasized the concept of spontaneous emission of light and demonstrated that electrons could be stimulated to emit radiation at specific wavelengths. With advancements in technology in recent years, modern lasers are capable of generating high intensity and coherent radiation across a wide spectral range from the infrared to the soft X-ray region. Moreover, laser beams can be easily directed and focused, and they can possess extremely high pulse energies, which allows for significant amplification of the optical output (Purohit, 2020).

The fundamental characteristics of laser light distinguish it from conventional light sources. Monochromaticity, brightness, high intensity, coherence, and directionality are its primary attributes. Due to these remarkable properties, lasers have found widespread applications across various domains from fundamental science and medicine to the manufacturing industry (Han et al., 2021; Bohacek, 2022; Flórez et al., 2023). On the other hand, due to the diverse characteristic properties of lasers, different laser types are preferred for various medical indications. Neodymium-doped yttrium aluminum garnet (Nd:YAG) lasers (Luke et al., 2019), CO_2 lasers (Parker, 2007), Argon lasers (Azadgoli and Baker, 2016), Q-switched ruby lasers (Bernstein and Adrian, 2006), Er:YAG lasers and Er:Glass lasers (Aslam and Alster, 2014) can be given as used lasers. Another laser type widely used in current dermatological applications is the Alexandrite laser (Yorulmaz et al., 2014). Solid-state lasers (SSLs), including Alexandrite lasers, are commonly employed in dermatology, clinical treatments, and various industrial applications. Alexandrite lasers are observed to provide high energy conversion efficiency for tissue absorption due to their optimal wavelength range. Additionally, their capability to adjust pulse duration and repetition rate contributes to increased overall efficiency. These features make Alexandrite lasers highly effective for both medical and cosmetic procedures (Šulc and Jelínková, 2013).

In lasers such as Alexandrite, amplification of the laser beam is required to generate coherent light emission.

This amplification process necessitates the presence of a resonant cavity within the laser system. The cavity also incorporates a cooling flow field. In other words, this section includes the crystal rod, resonator mirrors, and flash-lamps, integrated with optical diffuser materials and cooling inlets. It is commonly referred to as the optical cavity or pump chamber. The optical cavity serves as the chamber where light is optically pumped. One or more reflective surfaces are required to direct the pumped light toward the crystal rod (Svelto, 2010). Therefore, an elliptical reflector is included within the pump chamber, with the laser rod and flash-lamps positioned around each other's focal points. Through the optical pumping mechanism utilizing flash-lamps, the active medium is excited, thereby generating light emission. The geometry of the cavity determines whether it remains optically stable. This stability is directly linked to optical pumping efficiency, also referred to as optical conversion efficiency. In other words, this efficiency represents the effectiveness of a laser system in converting electrical energy into usable laser radiation. To enhance this efficiency, the cavity must be designed with an optimal geometric configuration (Hecht, 2018).

In the early commercial laser designs, pump chambers were constructed from polished, thermally conductive metals and benefited from specular reflection. However, due to the high cost and susceptibility to deformation of the gold and silver coatings used in these lasers, the system gradually evolved toward the utilization of diffuse reflection structures. Furthermore, only approximately 40%–50% of the light emitted from the lamps is absorbed, while the remainder is converted into heat. In laser applications, sequential pulsing is required and the generated heat must be dissipated for such pulses to occur efficiently (Svelto, 2010). To overcome this problem, specifically, the use of reflective powder materials was adopted to focus the reflected light multiple times and reduce scattered light (Mikhailov et al., 2021).

A review of the literature reveals that white quartz and barium sulfate $BaSO_4$ are commonly employed as diffuse reflector materials. For instance, Lawrence (2018) utilized pressure-molded barium sulfate material as an optical diffuser inside a metal housing containing a single lamp and a single crystal, to concentrate the flash-lamp's output and ensure its homogeneous distribution. In this laser configuration, only a portion of the light emitted from the lamps is absorbed, while the rest is transformed into heat. However, in Lawrence's system, cooling mechanisms were required to evacuate the high heat generated during sequential pulses. This necessity required the incorporation of cooling inlets into the design. In another study, Bavi et al. (2022) developed a white paint with a BaSO4-based pigment exhibiting diffuse reflectivity. They employed this paint as a back-surface reflector in photovoltaic cells and reported an increase in reflectivity up to 99%. Poh et al. (2019) conducted a spectroscopic analysis of diffuse reflection by comparing the pure and sintered forms of BaSO4. Examination of the current literature indicates that BaSO4 is widely used in powder coatings due to its high electrical conductivity and reflectivity properties.

On the other hand, the efficiency of laser light generation, pulse count, and overall energy performance depends not only on the reflective powders in pump chambers but also on the refractive index of the cavity framework materials. Materials with a low refractive index allow faster light propagation, influencing stimulated emission efficiency and causing the pumped light to spend less time inside the laser crystal. Therefore, fused silica is widely used in ultrafast laser systems despite its challenging micro-machinability. Studies demonstrate that fused silica microstructures can enhance femtosecond laser processing efficiency and that this material is also commonly employed in the cavity frameworks of solid-state lasers such as Alexandrite (Jian et al., 2021; Sun et al., 2009; Yang et al., 2023). In this context, Jian et al. (2021) conducted a study to improve processing methods in a femtosecond laser processing platform. For this operation, they used fused silica microstructures. Although femtosecond pulse generation was achieved using fused silica in their study, it was noted that machining the microstructure of the used silica was difficult (Jian et al., 2021). Yang et al. (2023) conducted an application involving the micro-milling of this material using fused silica in a 1030 nm femtosecond laser. It was reported that ablation efficiency was increased through milling of the cavities (Yang et al., 2023). In addition to these studies, it is observed that in the cavity framework of the Alexandrite laser, a solid-state optically pumped laser, fused silica with a high refractive index is commonly used (Sun et al., 2009).

In certain lasers, borosilicate glass has been preferred as an alternative to fused silica in order to prolong the use of light during the pumping process. This is due to the fact that borosilicate possesses a higher refractive index compared to fused silica.

In this context, Dharmadhikari et al. (2011) conducted a study utilizing borosilicate glass in laser applications. In their experiment, low-loss waveguides were inscribed in borosilicate (BK7) glass using a femtosecond laser, and the change in refractive index was measured. Li et al. (2020) induced nonlinear filamentation by directing an 800 nm femtosecond Bessel beam into a BOROFLOAT 33 borosilicate glass substrate. In this study, borosilicate glass was chosen for its high refractive index and reflective properties. In another study, to achieve high efficiency in femtosecond lasers, a diffraction grating was embedded inside a BK7 lens to focus the laser beam (Watanabe and Terai, 2020). In a different study, waveguides were formed in a femtosecond fiber laser by utilizing the focusing capability of BK7 on the laser beam (Wu et al., 2021). Overall, the optical properties of borosilicate glass make it a promising candidate for improving pulse efficiency and light confinement in various ultrafast laser configurations (Li et al., 2020;

Watanabe and Terai, 2020; Wu et al., 2021).

Building on the previous studies highlighting how cavity materials, refractive index properties, and reflective powders influence light confinement and pumping performance, flash-lamp-pumped solid-state lasers fundamentally rely on efficient conversion of electrical energy into optical output. Since only part of the pumped energy contributes to useful laser emission, while the rest becomes thermal loss, maximizing optical conversion efficiency is essential for achieving high output energy, reducing operational costs, and extending pulse lifetime. Motivated by the advantages and limitations of fused silica, borosilicate glass, and reflective materials reported in the literature, the present work focuses on enhancing the optical conversion efficiency of a solid-state Alexandrite laser, using a discontinued GentlelasePlus system (Candela, 2010) as the experimental platform.

The main contribution of the proposed study is as follows:

- The structure of the quartz framework in the optical pumping chamber is redesigned, distinguishing this work from existing studies in the literature. Specifically, the conventional three-hole skeleton made from fused silica glass is replaced with one fabricated using borosilicate (BK7).
- Using BK7, laser pulses are generated on the platform, energy outputs were measured, and optical conversion efficiency is calculated.
- The results demonstrate that the selected material enhances conversion efficiency, reduces energy consumption, and extends the operational lifetime of the laser, which are contributing a novel approach to the field.

This paper is organized as follows: the characteristics of the discontinued and decommissioned GentlelasePlus Alexandrite solid-state laser are presented in Section 2. In this section, detailed information is also provided regarding the internal structure of the laser head used in the study, as well as the cavity framework designed with BK7, which constitutes the cavity structure. Additionally, the parameters required to calculate the optical conversion efficiency are mathematically defined. The results are presented with tables and graphs in Section 3. This study is also compared with those reported in existing studies in the literature in Section 4 called as Discussion. Finally, the paper concludes with Section 5 titled Conclusion. The limitation and future works are also discussed in Section 6.

2. Materials and Methods

2.1. Laser System

Optical conversion efficiency (OCE) varies depending on several factors, including the laser gain medium, pump source, and cavity geometry. Among these, the optical cavity enhances photon density through their oscillation between mirrors, a process that occurs within reflective chambers where laser emissions are amplified. In short, the usage of a reflective chamber is essential to improving a laser's optical conversion efficiency.

In the literature, the optical cavity is defined as the region between the laser's end mirrors, including the mirrors themselves. In practice, it refers to the structure that houses the crystal rod, mirrors, and flash-lamps, equipped with optical diffuser materials and integrated cooling inlets. This structure is referred to as the optical cavity or pump chamber and is located within the metal enclosure of the laser head. Within this head, the reflective optical diffuser is any material that scatters or redistributes incident light uniformly in all directions through small scattering centers, providing uniform illumination and reduced intensity. Reflective diffusers scatter light backward from opaque surfaces, while transmissive diffusers forward-scatter light through transparent media.

In this study, the OCE of a solid-state laser is enhanced by modifying the properties of its optical cavity. The objective is to reduce energy consumption and increase pulse lifetime. For this purpose, a discontinued and decommissioned Gentlelaseplus Alexandrite solid-state (AS-S) laser is used (Candela, 2010). The technical specifications of the laser are presented in Table 1.

Table 1. Technical specifications of the Gentlelaseplus Alexandrite solid-state (AS-S) laser (Candela, 2010)

Specifications	Application Values
Laser Type	Flash-lamp-pumped, pulsed (AS-S)
Wavelength	755 nm
Maximum Transmitted Energy	53 (J)
Output Energy Accuracy	± 20%
Pulse Repetition Rate	1 Hz
Pulse Duration	3 ms
Voltage and Power	200 V- 240V, 50/60 Hz, single phase, 4.600 VA

Figure 1 shows the laser head of the Gentlelaseplus Alexandrite solid-state laser system. The green area depicted in Figure 1 presents the general block diagram of the laser head used in this study. In this configuration, the optical path of the light generated within the laser head is illustrated. The yellow-highlighted area provides a detailed view of the internal structure, which consists of the optical diffuser forming the cavity framework. The optical diffuser, also referred to as the triple bore, supports both the lamps and the rod. Additionally, this

component serves as the primary reflective region. The optical diffuser used in this study comprises three holes.

In the blue area shown in Figure 1, the placement of the optical diffuser inside the laser head is illustrated. The Alexandrite crystal rod is positioned in the central bore of the diffuser. The location and structure of this rod are clearly depicted in the yellow highlighted section. The Alexandrite crystal rod used in this study operates at a wavelength of 755 nm and has a cylindrical geometry with a diameter of 9.52 mm and a length of 115 mm. The mirrors at both ends of the crystal are specially fabricated and integrated with anti-reflective coatings. The high-reflectivity mirror has a reflectance of 99.9%, while the partial reflector exhibits a reflectance of 81.5%.

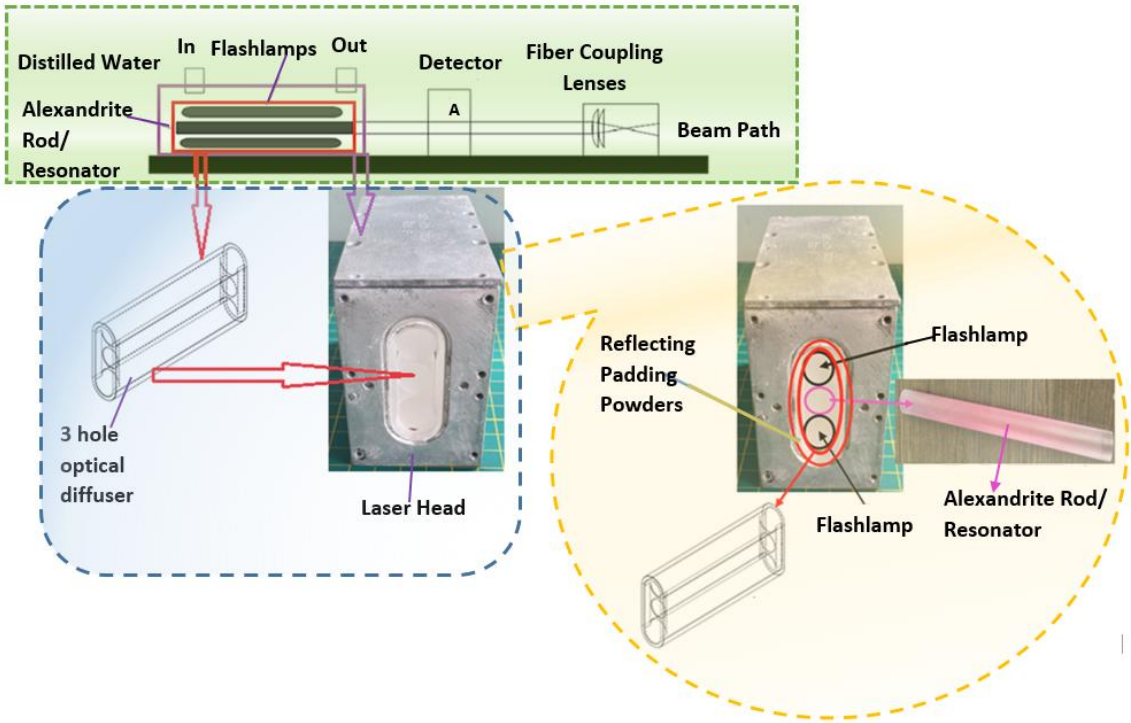

Figure 1. Laser head block diagram.

On the other hand, a reflective filler powder is placed between the metal block structure (or the metal housing of the laser head) and the optical diffuser. The region containing the filler powder (white powder) is located between the two red cylindrical areas within the yellow dashed area shown in Figure 1. When light passes through an optical diffuser, its direction changes multiple times at the diffuser surface. This process causes the light to scatter at different angles, resulting in a homogeneous light distribution. The flash-lamps are positioned in the upper and lower bores of the optical diffuser, and their placement is illustrated in the yellow-highlighted section of Figure 1. Furthermore, the positioning of the flash-lamps inside the laser head and the corresponding light output points are also presented in Figure 2.

When the flash-lamps in the electrical system of the laser are driven within the range of 900–2000Vdc, laser output energy is generated. To obtain a more efficient and stable output from the gain medium of the system, it is maintained in thermal equilibrium using cooling water at 60°C. Figure 3 presents the circuit diagram of the electrical system used to drive the flash-lamps.

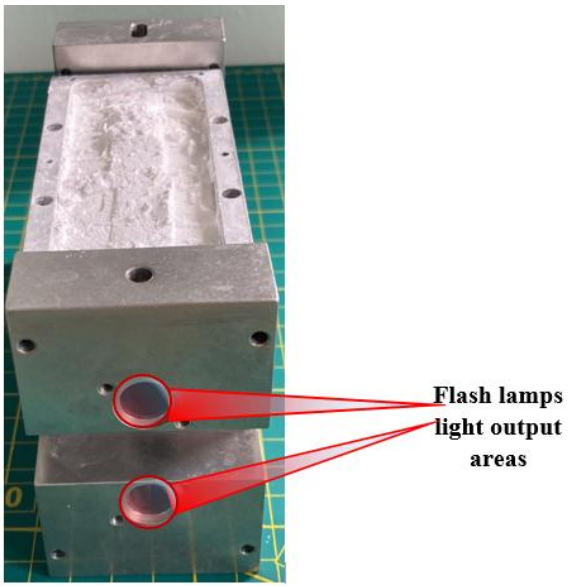

Figure 2. The exit areas of the light from the flash-lamps on the laser head.

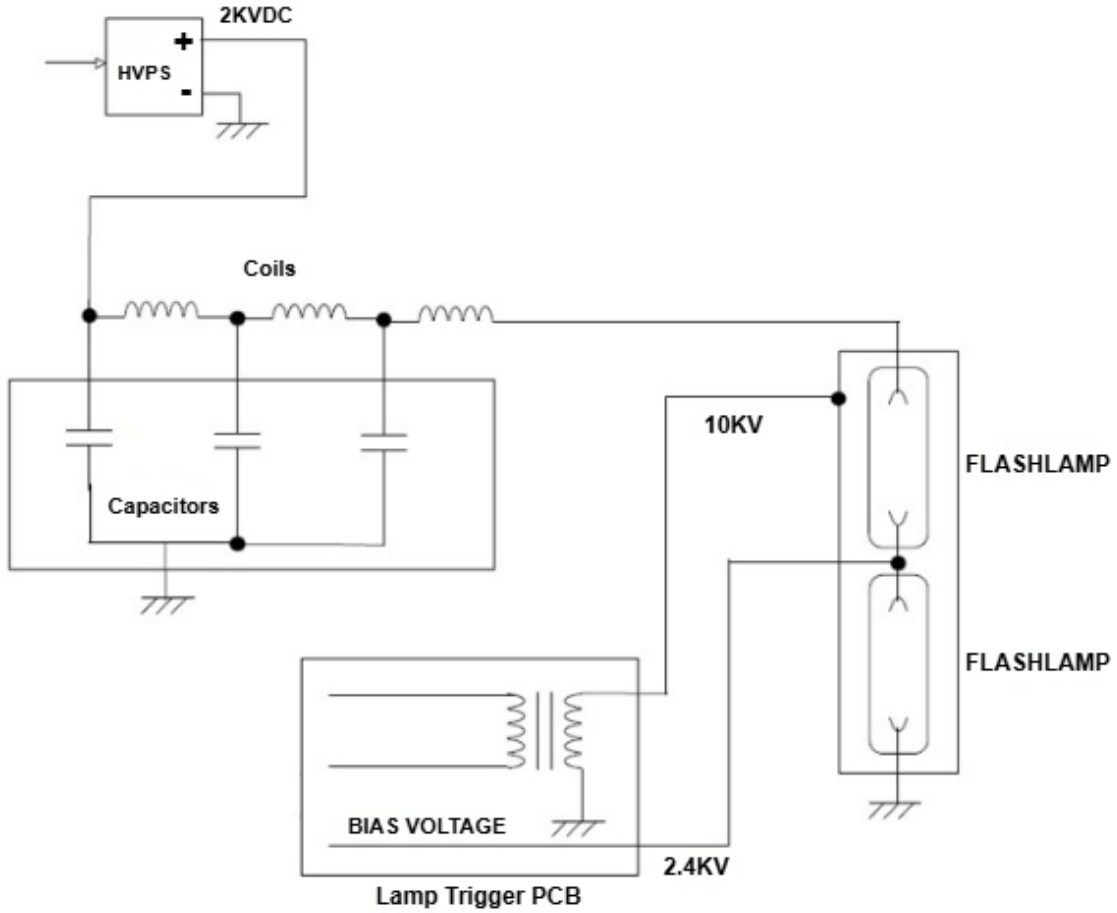

Figure 3. The circuit diagram of the electrical system.

In the electrical system of the laser, three parallel connected capacitors and three series connected inductors are used. The capacitance value of each capacitor (C) is $550X10^{-6}F$, while the inductance values of the inductors (L) are 750 μH , 450 μH, and 300 μH, respectively. In this context, the total capacitance and inductance are calculated as 183.33 μH and 1500 μH, respectively. On the other hand, when the flash-lamps are driven within the range of 900-2000 Vdc, the peak current obtained in the system is determined according to the equation 1 (Almabouada et al., 2011).

$$I_{peak} = \frac{V}{\sqrt{\frac{L}{C}}} \tag{1}$$

Based on the peak current, the pumping power (P_{pump}) obtained from the system is calculated using the equation 2. The unit of power is Watt (W). The pumping energy (E_{pump}) is equal to the product of the pumping power and the pulse duration (t). (See equation 3). The unit of pulse duration is second.

$$P_{pump} = V * I_{peak} \tag{2}$$

$$E_{pump} = P_{pump} * t \tag{3}$$

In the expression of energy density, the electrical energy consumed in a single pulse is also referred to as pumping energy. On the other hand, this energy is also required for calculating the OCE. As mentioned above, OCE is defined as the ratio of the energy measured in the form of a laser beam (E_M) to the pumping energy expended to generate this beam. In equation 4, the gain expression representing the optical conversion efficiency (η_{OCE}) is mathematically formulated (Eichler et al., 2005).

$$\eta_{OCE} = \frac{E_M}{E_{pump}} * 100(\%) \tag{4}$$

The overall efficiency ($\eta_{overall}$) of the system is determined by the ratio of the output energy measured at the laser output to the electrical energy (E_{MLO}) supplied to the system expression is given in equation 5.

$$\eta_{overall} = \frac{E_M}{E_{MLO}} * 100(\%) \tag{5}$$

2.2. Materials

Laser amplification requires a minimum of three energy levels. Three-level lasers, such as the ruby laser, are characterized by short transition lifetimes and a relatively high pumping energy requirement. Population inversion is achieved by optically pumping atoms to higher energy levels and maintaining them for a sufficient duration in a metastable state, while laser emission occurs through transitions between specific energy levels. The depopulation of an energy level can take place either via photon emission or through non-radiative relaxation mechanisms associated with atomic

interactions such as collisions or vibrational processes (Hecht, 2018). In this study, the gain medium is a solid-state laser incorporating an Alexandrite crystal, which operates as a four-level laser system in which the laser transition does not terminate at the ground state, and the emitted output power is described by the four-level laser power expression given in equation 6 (Yariv, 1991).

$$(P)_{4level} = \frac{8\pi n^3 h \Delta v V}{\lambda^3 t_c} \frac{t_{spont}}{t^2} \quad (6)$$

In this equation, the parameters n, h, v and V denote the refractive index, Planck's constant, the spectral bandwidth, and the volume of the gain medium, respectively. In addition, the wavelength is represented by λ. The parameters t_{spont} and t^2 correspond to the spontaneous emission lifetime and the square of the characteristic time, respectively. On the other hand, t_c is defined as the cavity lifetime, representing the average residence time of a photon within the laser cavity, and its value is mathematically expressed in equation 7.

$$t_c \cong \frac{nl}{(1-R)c} \quad (7)$$

Here, c denotes the speed of light, and R represents the reflectivity of the cavity mirrors.

As discussed in the previous section, the pulse duration (t) directly affects the temporal distribution of the pumping energy and, consequently, the optical conversion efficiency. In flash-lamp–pumped laser systems, the amplitude and duration of the applied electrical pulse determine the radiant flux emitted by the lamp and thus govern the level of population inversion established in the gain medium. In this study, the pumping conditions were electronically controlled using a 3 ms pulse duration.

The cavity lifetime (t_c), defined as the average residence time of a photon inside the laser cavity, depends on the mirror reflectivities and total cavity losses, and constitutes a key parameter influencing the overall energy efficiency of the laser system. In addition, t_{spont} represents the spontaneous emission lifetime, while t^2 corresponds to the square of the characteristic time constant of the gain medium. These parameters collectively define the temporal dynamics of laser emission and output energy.

In order to isolate and simplify the influence of cavity-related effects, the laser system was modeled as a closed reflective enclosure while maintaining constant pumping conditions. Under these controlled conditions, only the cavity reflective element was varied. This approach enabled a direct assessment of how a single component modification affects the laser output, rather than analyzing the combined influence of multiple system parameters. Accordingly, the cavity performance was evaluated solely on the basis of the diffraction and scattering characteristics of the reflective powder coating employed in the cavity design, while all other system parameters were assumed to remain constant.

In this context, in line with the experimental system described above and the mathematical expressions provided, the material forming the cavity framework in the laser head is modified to improve the OCE. In this context, borosilicate (BK7) glass is used instead of quartz in the framework structure. The cavity skeleton is constructed with a three-bore optical diffuser reflector fabricated from BK7. On the other hand, in the comparative evaluation of cavity frames fabricated from BK7 and quartz materials, identical flash-lamps are deliberately employed to eliminate pump source related variability. Moreover, beyond the flash-lamps, all remaining components associated with the crystal rod assembly and the laser head architecture was strictly kept identical for both BK7 and quartz based configurations. Accordingly, controlled pulsed operation was applied to the laser platform, and the resulting output pulse energies were quantitatively measured using a calibrated laser energy meter, after rigorously ensuring that any observed performance differences could be attributed exclusively to the cavity frame material. Since all components of the cavity structure, which are except for the reflective powder, are maintained identical, secondary influences such as component aging and thermal drift did not require separate consideration. Lamp degradation, which is including contamination and burn-in on the flash-lamp, typically becomes pronounced only after extended operation exceeding approximately 1000 pulses. As the experimental process in this study was limited to 35 pulses for both cavity materials, component aging and flash-lamp degradation phenomena are therefore considered negligible and have not been evaluated independently.

To explain the reason for preferring BK7 glass in this study, it is first necessary to define the concept of refractive index and emphasize its importance in selecting the glass material for the cavity framework. The refractive index (η), mathematically defined in equation 8, is the ratio of the velocity of light wave in free space (c) to its velocity in a medium (v), and as this index increases, the velocity decreases (Cheng, 2017).

$$n = \frac{c}{v} \quad (8)$$

All glasses used in the pump chamber are classified into two categories as crown glass and flint glass. Flint glass (FG) exhibits strong chromatic dispersion and a high refractive index. In addition, its optical Abbe number (AN) is less than 50 (AS < 50). In contrast, crown glasses generally have a lower refractive index (RI) and an Abbe number greater than 50 (AS > 50). The refractive index of BK7 at 587.6 nm is 1.5168 with an Abbe number of 64.17. Similarly, fused silica, also a crown glass, has a refractive index of 1.4584 and an Abbe number of 67.8. In addition, the transmitted wavelength range (TWR) values are the same for both glass types, ranging from 587.6 nm to 780 nm (Polyanskiy, 2024).

In this study, a glass material with an elevated refractive index is selected for the pump chamber in order to reduce the group velocity of the pump radiation, thereby increasing its interaction time within the cavity and enabling higher output power at lower pumping energies. In this context, the usage of BK7 glass is proposed. To clarify the reason for preferring BK7, it was compared with the commonly used quartz glass. Table 2 presents the properties of BK7 and quartz glass.

In Figure 4 (a), the three-bore optical diffuser (cavity framework) designed in this study using BK7 is presented, while Figure 4 (b) shows the images of quartz and BK7. In the image given in Figure 4 (b), the white glass corresponds to quartz, which has widespread use in the literature. The transparent glass represents BK7. The cavity framework fabricated from BK7 and shown in Figure 4 (a) was produced for the first time within the scope of this study. The application of the three-bore BK7 cavity framework in the laser head is clearly illustrated in Figure 1.

Table 2. Comparison of BK7 and quartz glass

	TWR* (nm)	RI* (n)	Transmittance (%)	AN*
BK7	587.6 nm – 780 nm	1.5168 – 1.512	92	64.17
Quartz	587.6 nm – 780 nm	1.4584 – 1.46	94	67.80

TWR= transmitted wavelength range, RI= refractive index, AN= abbe number

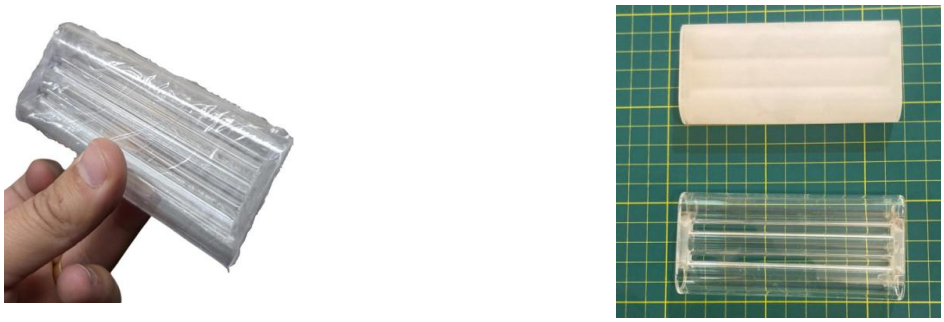

(a) (b)

Figure 4. Cavity framework images. (a) BK7 glass; (b) Quartz and BK7 glass.

3. Results

In this study, conducted to improve the OCE, the results obtained from the laser system operated with the cavity framework fabricated from BK7 are presented. During the experiments, all components in the existing laser head are used in their original form, with the only modification being the replacement of the glass material in the cavity framework. Accordingly, results are obtained both for the original quartz glass and for the three-bore framework fabricated from BK7 within the scope of this study.

In the electrical system of the laser, the flash-lamps are driven at voltages of 900 Vdc and 1070 Vdc to generate radiation. When the flash-lamps are operated at 900 Vdc, the measured laser output energy (E_{MLO}) is 1 J. The pumping energy, calculated using Equations 1 - 3, is 849.5400 1 J at this voltage. At 1070 Vdc, the E_{MLO} reached 10 J, while the corresponding pumping energy is 1200.8000 J. The values of E_{pump} are determined by considering pulse durations of $t = 0.003$ seconds, with peak currents of 630 A at 900 Vdc and 749 A at 1070Vdc. The peak currents are calculated based on the total capacitance and inductance values in the system.

To clearly observe the variation in energy measurement, the flash-lamps are first driven at 900Vdc, and the energy generated in the form of a laser beam (E_M) was recorded. The experimental procedure is repeated 35 times to obtain reliable E_M values. This process is conducted separately for each of the two cavity framework materials. In other words, 35 laser pulses are produced for both materials, and E_M is measured at each step. Based on the measured values, the optical conversion efficiency (η_{OCE}) is calculated. All results are presented in Table 3.

The graphical representation of the values listed in Table 3 is presented in Figure 5. Figure 5 (a) illustrates the E_M results obtained for 35 laser pulses. To facilitate a more accurate interpretation of both the graph and the table, the measurement values were reordered in ascending order and are presented in Figure 5 (b).

Based on the measured E_M values, the η_{OCE} is also calculated in this study. A comparative graphical representation of these results, presented in Table 3, is illustrated for the two materials in Figure 6.

In laser systems, the optical output of the flash-lamps varies with the applied voltage. Higher applied voltage results in an increase in both light intensity and output power, thereby leading to greater energy generation. As illustrated in Figure 5 and Figure 6, the measurement energy (E_M) values exhibit a direct correlation with the corresponding optical conversion efficiency, where higher η_{OCE} values are associated with increased E_M.

On the other hand, when the average E_M values obtained over 35 laser pulses are examined, 1.1708 J is measured for Quartz and 1.0216 J for BK7. The corresponding average η_{OCE} are calculated as 0.1378% and 0.1203 % for

Quartz and BK7, respectively. These results indicate that the energy performance of the two materials is comparable, suggesting that BK7 may serve as an alternative to Quartz. To further substantiate this assumption, the applied voltage to the flash-lamps is increased and the results are re-evaluated. In this context, a second experimental condition was established by applying 1070 Vdc to the flash-lamps, at which an output energy of 10 J was obtained, consistent with the observations mentioned earlier. At this voltage level, the calculated pumping energy E_{pump} is 1200.8000 J. Table 4 presents the average E_M values obtained over 35 pulses under 1070 Vdc (10 J) excitation. In addition, the table also reports the corresponding η_{OCE} calculated for Quartz and BK7, respectively.

The graphical comparisons of the E_M values and the η_{OCE} obtained for both materials, based on the data presented in Table 4, are illustrated in Figure 7. These plots are generated by arranging the datasets corresponding to 35 laser pulses in ascending order.

Table 3. E_{pump}, E_M, and η_{OCE} obtained by operating the flash-lamps at 900 Vdc (1 J)

Pulse Number	E_{pump} (J)	E_M obtained with Quartz (J)	η_{OCE}(%) (Quartz)	E_M obtained with BK7 (J)	η_{OCE}(%) (BK7)
Pulse 1	849.4500	1.1400	0.1342	0.9880	0.1163
Pulse 2	849.4500	1.3060	0.1537	0.9900	0.1165
Pulse 3	849.4500	1.1360	0.1337	1.0840	0.1276
Pulse 4	849.4500	1.2550	0.1477	1.0760	0.1267
Pulse 5	849.4500	1.1370	0.1338	0.9950	0.1171
Pulse 6	849.4500	1.0840	0.1276	1.0400	0.1224
Pulse 7	849.4500	1.1250	0.1324	1.0800	0.1271
Pulse 8	849.4500	1.1900	0.1401	0.9860	0.1161
Pulse 9	849.4500	1.1150	0.1312	0.9960	0.1172
Pulse 10	849.4500	1.2000	0.1413	0.9800	0.1154
Pulse 11	849.4500	1.0200	0.1201	0.9830	0.1157
Pulse 12	849.4500	1.1250	0.1324	0.9900	0.1165
Pulse 13	849.4500	1.0370	0.1221	0.9840	0.1158
Pulse 14	849.4500	1.0840	0.1276	1.0860	0.1278
Pulse 15	849.4500	1.1900	0.1401	0.9850	0.1159
Pulse 16	849.4500	1.2060	0.1420	1.0400	0.1224
Pulse 17	849.4500	1.3360	0.1573	0.9800	0.1154
Pulse 18	849.4500	1.2560	0.1478	1.0770	0.1268
Pulse 19	849.4500	1.0700	0.1260	0.9960	0.1172
Pulse 20	849.4500	1.0900	0.1283	0.9800	0.1154
Pulse 21	849.4500	1.0771	0.1268	0.9820	0.1156
Pulse 22	849.4500	1.0864	0.1279	0.9854	0.1160
Pulse 23	849.4500	1.0966	0.1291	0.9879	0.1163
Pulse 24	849.4500	1.1315	0.1332	0.9930	0.1169
Pulse 25	849.4500	1.1527	0.1357	1.0015	0.1179
Pulse 26	849.4500	1.1663	0.1373	0.9981	0.1175
Pulse 27	849.4500	1.0576	0.1245	0.9769	0.1150
Pulse 28	849.4500	1.1875	0.1398	1.0125	0.1192
Pulse 29	849.4500	1.1969	0.1409	1.0499	0.1236
Pulse 30	849.4500	1.2181	0.1434	1.0219	0.1203
Pulse 31	849.4500	1.2835	0.1511	1.0915	0.1285
Pulse 32	849.4500	1.2997	0.1530	1.0941	0.1288
Pulse 33	849.4500	1.2326	0.1451	1.0440	0.1229
Pulse 34	849.4500	1.3421	0.1580	1.0975	0.1292
Pulse 35	849.4500	1.3481	0.1587	1.1026	0.1298
The average values obtained from 20 laser pulses	849.4500	1.1708	0.1378	1.0216	0.1203

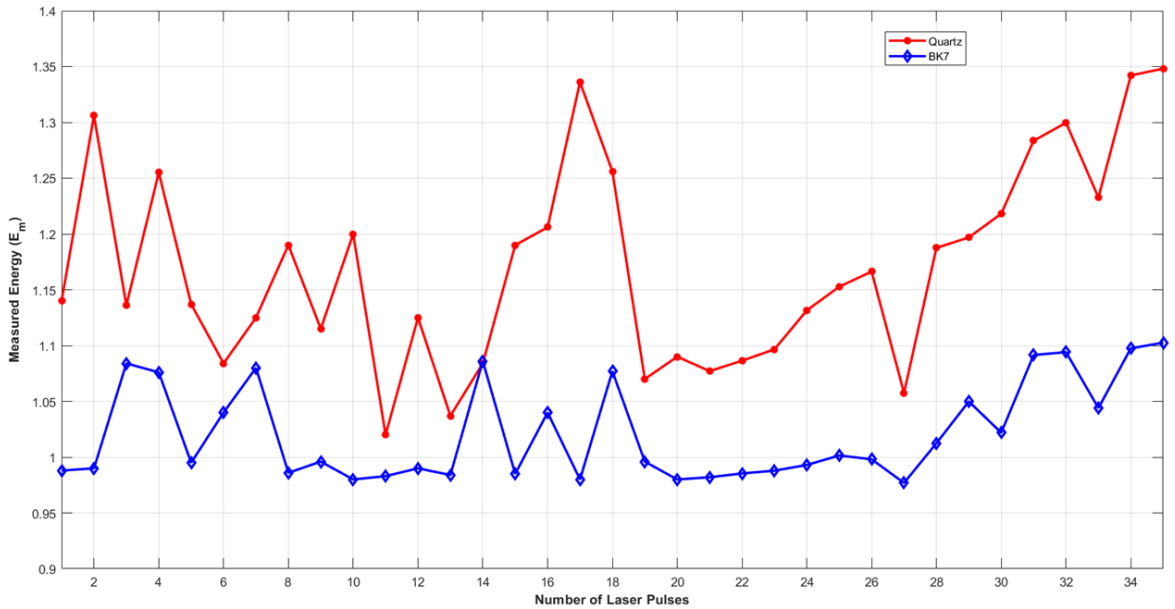

(a)

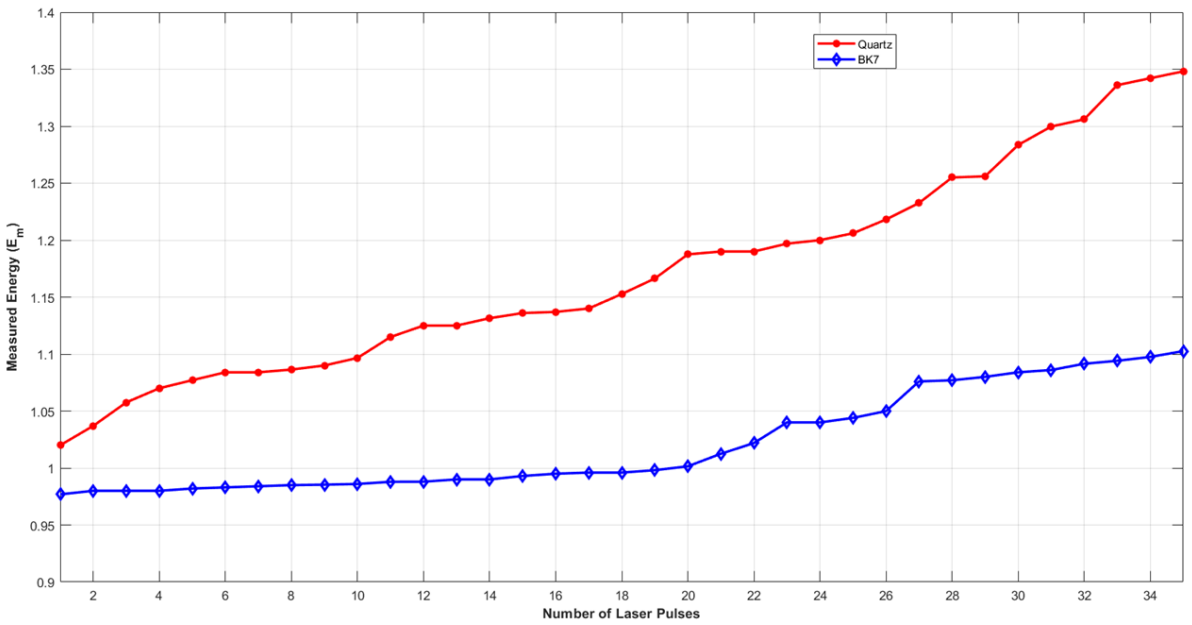

(b)

Figure 5. E_M values obtained from 20 laser pulses employing resonator structures constructed from Quartz and BK7 at 900 Vdc (1 J) pulse energy. (a) Raw data distribution; (b) Values arranged in ascending order.

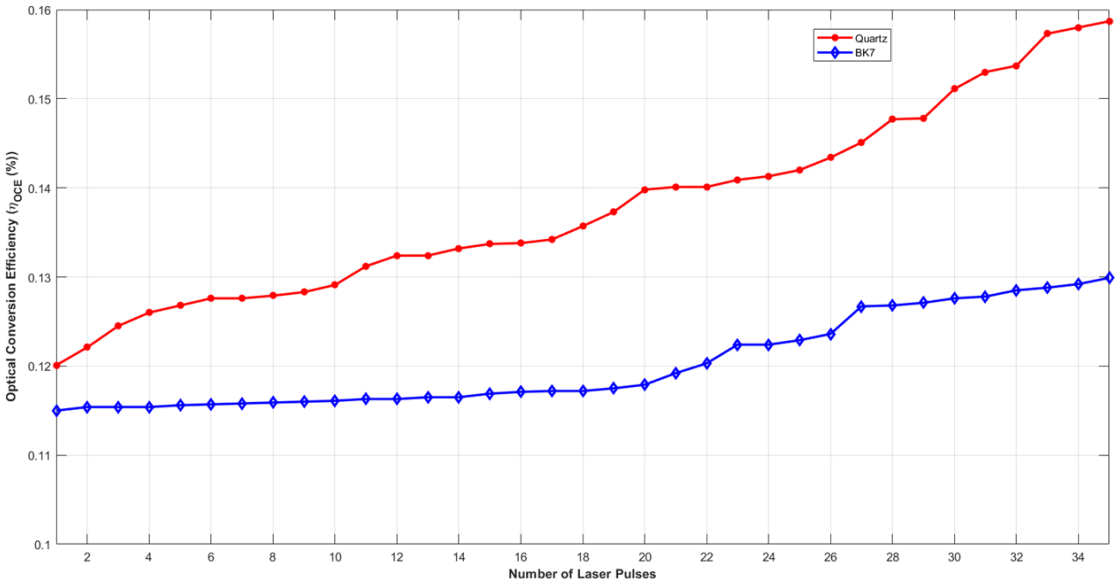

Figure 6. Comparison of the η_{OCE} values obtained for Quartz and BK7 at 900 Vdc (1 J). (arranged in ascending order).

Table 4. E_{pump}, E_M, and η_{OCE} obtained by operating the flash-lamps at 1070 Vdc (10 J).

Pulse Number	E_{pump} (J)	E_M obtained with Quartz (J)	η_{OCE}(%) (Quartz)	E_M obtained with BK7 (J)	η_{OCE}(%) (BK7)
Pulse 1	1200.8000	10.9800	0.9144	11.4500	0.9535
Pulse 2	1200.8000	10.6700	0.8886	11.4400	0.9527
Pulse 3	1200.8000	10.8800	0.9061	11.3200	0.9427
Pulse 4	1200.8000	10.8200	0.9011	10.8800	0.9061
Pulse 5	1200.8000	10.6400	0.8861	11.2200	0.9344
Pulse 6	1200.8000	10.3800	0.8644	11.4200	0.9510
Pulse 7	1200.8000	11.0100	0.9169	11.1600	0.9294
Pulse 8	1200.8000	10.2700	0.8553	11.2700	0.9385
Pulse 9	1200.8000	10.4700	0.8719	10.9500	0.9119
Pulse 10	1200.8000	10.6200	0.8844	11.8200	0.9843
Pulse 11	1200.8000	10.7100	0.8919	11.8800	0.9893
Pulse 12	1200.8000	10.1400	0.8444	10.9900	0.9152
Pulse 13	1200.8000	10.3400	0.8611	11.3000	0.9410
Pulse 14	1200.8000	10.7100	0.8919	11.0900	0.9236
Pulse 15	1200.8000	10.1700	0.8469	10.9700	0.9136
Pulse 16	1200.8000	10.9500	0.9119	11.3400	0.9444
Pulse 17	1200.8000	11.1600	0.9294	11.1300	0.9269
Pulse 18	1200.8000	11.2200	0.9344	11.3200	0.9427
Pulse 19	1200.8000	11.3200	0.9427	10.9400	0.9111
Pulse 20	1200.8000	10.7200	0.8927	11.6700	0.9719
Pulse 21	1200.8000	10.1492	0.8452	10.9045	0.9081
Pulse 22	1200.8000	10.1960	0.8491	10.9441	0.9114
Pulse 23	1200.8000	10.5947	0.8823	11.1038	0.9247
Pulse 24	1200.8000	10.3725	0.8638	10.9861	0.9149
Pulse 25	1200.8000	10.6115	0.8837	11.1134	0.9255
Pulse 26	1200.8000	10.7424	0.8946	11.3235	0.9430
Pulse 27	1200.8000	10.8372	0.9025	11.3259	0.9432
Pulse 28	1200.8000	10.4434	0.8678	10.9993	0.9160
Pulse 29	1200.8000	10.4350	0.8690	11.0462	0.9199
Pulse 30	1200.8000	11.0197	0.9177	11.4676	0.9550
Pulse 31	1200.8000	11.0245	0.9181	11.5277	0.9600
Pulse 32	1200.8000	11.4232	0.9513	11.8867	0.9899
Pulse 33	1200.8000	11.4881	0.9567	11.9984	0.9992
Pulse 34	1200.8000	10.7243	0.8931	11.3139	0.9422
Pulse 35	1200.8000	11.2887	0.9401	11.8363	0.9857
The average values obtained from 20 laser pulses	1200.8000	10.7294	0.8935	11.2954	0.9407

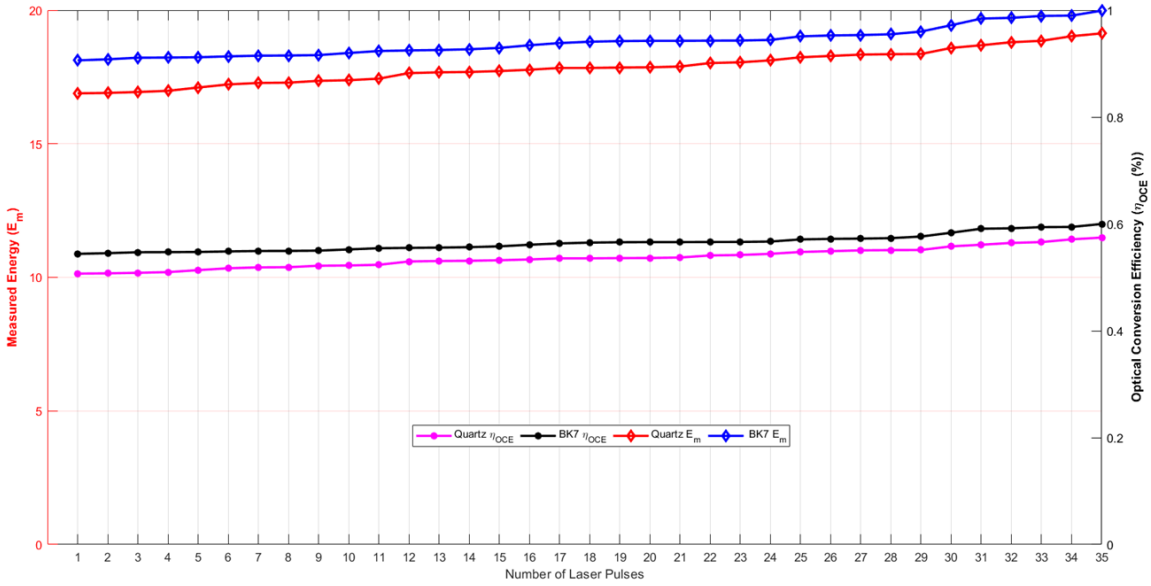

Figure 7. Comparison of the E_M and η_{OCE} values obtained for Quartz and BK7 at 1070 Vdc (10 J). (arranged in ascending order).

When the flash-lamps are driven with 1070Vdc, the higher radiative output obtained with the BK7 material is evident in Table 4 and Figure 7. The average E_M values calculated over 35 laser pulses is 10.7294 J for quartz and 11.2954 J for BK7. It is indicating that both optical materials enabled the flash-lamp pumped system to exceed the nominal 10 J output energy required for stable operation. This enhancement directly influences the overall optical conversion efficiency. On the other hand, the average η_{OCE}values are computed as 0.8935 J and 0.9407 J for quartz and BK7, respectively. It demonstrates that the BK7 element provides approximately a 0.047 increase in efficiency relative to quartz. The experimental data associated with these performance metrics are summarized in Table 5. According to Table 5, the optical conversion efficiency achieved with BK7 at low pump energy (1 J) is lower than that obtained with quartz. However, the operational baseline of the Alexandrite laser used for the experimental measurements is 10 J and the primary parameter determining this operating point is the flash-lamp drive voltage. Thus, the η_{OCE} values computed at 1 J naturally indicate a lower efficiency for BK7 under low-voltage excitation (0.1203 < 0.1378). At higher flash-lamp voltages, which is corresponding to 10 J, the higher η_{OCE} obtained with BK7 relative to quartz represents the intended performance outcome of this study (0.9407 > 0.8935).

Table 5. General performance evaluation

Voltage (Vdc)	$I_{peak}(A)$	$I_{peak}(A)$	E_M (J)	$\eta_{OCE}(\%)$	$\eta_{OCE}(\%)$
900	630	849.5400	1.1708	0.1378	Quartz
900	630	849.5400	1.0216	0.1203	BK7
1070	749	1200.8000	10.7294	0.8935	Quartz
1070	749	1200.8000	11.2954	0.9407	BK7

In addition to the results presented above, the mean values and the corresponding standard deviations were calculated for the voltage level of 1070 Vdc. The values obtained from 35 laser pulses are presented in Figure 8.

On the other hand, it should be emphasized that the lower efficiency observed in the low-fluence regime does not indicate a limitation or malfunction of the laser system used in this study. The laser device can be operated at reduced high-voltage levels for testing and maintenance purposes. However, under standard user-mode operation, the system is designed to function within a fluence range of 10–30 J/cm, where a fluence of 10 J/cm corresponds to an output energy of approximately 25 J. Consequently, the lack of performance at low joule levels arises from operation outside the nominal working regime and does not reflect any intrinsic deficiency of the laser device used in the experiments.

Furthermore, the η_{OCE} in flash-lamp pumped solid-state lasers rarely exceeds 1 (%) (Arieli, 2025; Garrec, 2010). Therefore, the optical conversion efficiencies measured in this work are consistent with the expected behavior of flash-lamp driven pumping architectures. As a result, the optical conversion efficiency of BK7 is higher than that of quartz. This indicates that BK7 can be reliably employed as an alternative optical material in the cavity design of the existing Alexandrite laser system.

Obtaining the η_{OCE} values within the scope of this study

is essential for quantifying efficiency. The findings indicate that the optical cavity efficiency can be enhanced through a single material substitution. However, this improvement is not limited solely to the η_{OCE} parameter. Accordingly, the contribution of the material changed to the overall laser system efficiency at high energy levels is also examined. Based on the average E_M values measured over 35 successive pulses, a 7 % increase in output energy is achieved when using quartz, whereas a 13 % increase is obtained with BK7. Consequently, at elevated operating voltages, the energy generated in the newly designed BK7 based pump chamber is observed to be 6 % higher than that of the quartz-based chamber. In other words, the overall efficiency ($\eta_{overall}$) increased by approximately 13 % when the optical cavity framework is fabricated using BK7 material.

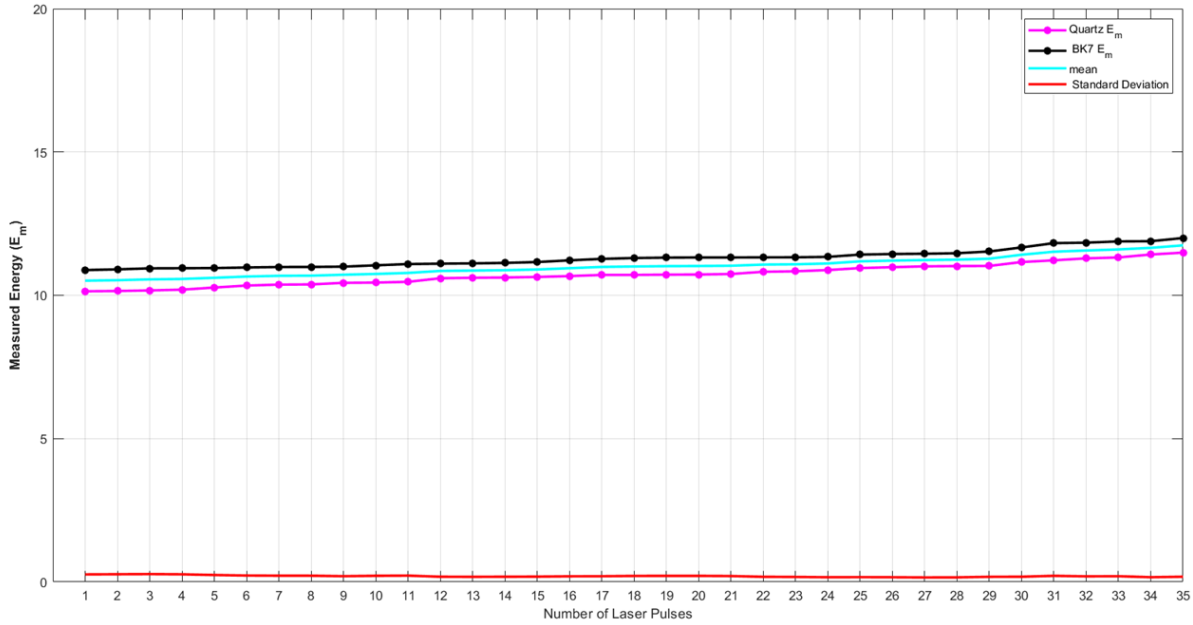

Figure 8. The mean values and the corresponding standard deviations for 35 laser pulses at 1070 Vdc (10 J).

4. Discussion

Extensive studies have been conducted in the literature to investigate optical conversion efficiency (η_{OCE}), slope efficiency, and overall efficiency ($\eta_{overall}$) in laser systems. However, the pumping schemes and efficiency optimization approaches employed in these studies vary significantly. In this study, a comparison with existing literature is provided to demonstrate that the use of BK7 as the optical cavity frame material in an Alexandrite laser has been implemented for the first time and to highlight the high efficiency performance achieved. The state of the existing studies is summarized in Table 6.

Garrec investigated the impact of laser diode and flash-lamp pumping on the efficiency of solid-state lasers. He emphasized that flash-lamp pumping is considered an outdated technology, while diode pumping offers several advantages in comparison. However, he also noted that flash-lamp-pumped fusion lasers exhibit high beam quality and high harmonic generation efficiency. Nevertheless, he stated that the overall laser efficiency in flash-lamp-pumped solid-state lasers has rarely exceeded 1 % (Garrec, 2010).

Unland et al. (2023) conducted a study to develop a Q-switched Alexandrite laser, aiming to achieve high-performance and high-efficiency short-pulse laser output. In this context, they implemented a continuous-wave (CW), double-pass diode-pumped, cavity-dumped Q-switching scheme. Additionally, they employed an L-shaped laser resonator configuration for pumping. However, no modifications were made to the cavity frame material in this study. The results were obtained using two similar Alexandrite laser crystals with different Cr^{3+} doping concentrations. The reported efficiency in the referenced study refers specifically to slope efficiency (SE), and no data were provided regarding η_{OCE}.

Song et al. (2021) investigated the enhancement of optical conversion efficiency (OCE) and SE in a 755 nm continuous-wave (CW) Alexandrite laser by pumping with laser diodes (LDs) operating at different wavelengths. In this context, 638 nm and 532 nm wavelength LDs were individually used for single-end pumping. Alexandrite lasers pumped at these wavelengths were comparatively analyzed. In other words, flash-lamp pumping is not employed in this study, and no modifications were made to the optical cavity frame. The η values were determined specifically for the LDs used in the pumping process. The study also demonstrated that a double-end pumped Alexandrite laser using fiber-coupled 638 nm LDs achieved opticalto-optical conversion efficiency (OtO-E) and SE of 16.3 % and 24.2 %, respectively, at 755 nm.

Scheuer et al. (2024) investigated the efficiency (η_{OCE}) of an Alexandrite ring laser by employing pumping with a frequency-doubled in intracavity, Qswitched diode source. The laser emitted direct ultraviolet (UV) radiation at 386 nm and the pumping process was

implemented using a fiber-coupled diode module. The Alexandrite crystal utilized in the study contained 0.2 % Cr^{3+} dopant concentration and was incorporated within a ring resonator configuration, without any structural modifications to the optical cavity. The reported optical-to-optical efficiency (OtO-E) of the UV laser exceeded 9%. Xiao and Damzen conducted a study on wavelength tuning of diode pumped Alexandrite lasers operating in the ultraviolet (UV) spectral region. In this context, cavity analysis was performed for the resonator design, based on Magni's intracavity lens mode-size model. The Alexandrite crystal employed in the cavity was mounted in a temperature-controlled metallic crystal holder, with the operating temperature stabilized at $25^{\circ}C$. The achieved optical efficiency in this study was 16.2 %. However, the misalignment of mirrors and the reliance on a temperature-controlled crystal mount within the cavity were identified as potential drawbacks (Xiao and Damzen, 2024).

Table 6. The state of the existing studies

Reference	Laser Type	Pump Source	Wavelength	Efficiency Type	Efficiency
Garrec (2010)	Solid State Laser	Laser-diode and Flash-Lamp Pumped	-	Overall laser efficiency	< 1 %
Unland et al. (2023)	CW Alexandrite laser	Diode-pumped	-	Slope efficiency	36 %
Song et al. (2021)	Alexandrite lasers	Laser diodes (LDs)	755 nm	Optical-to-optical conversion efficiency and slope efficiency	16.3 % and 24.2 %
Scheuer et al. (2024)	Q-switched diode-pumped alexandrite ring-laser	Diode-pumped	386 nm	Optical-to-optical efficiency	> 9 %
Xiao and Damzen (2024)	Continuous-wave wavelength-tunable Alexandrite lasers	Diode-pumped	38 nm to 402 nm	Optical-to-optical efficiency	16.2 %
Tawy et al. (2023)	Continuous-wave Alexandrite lasers	Fibre-coupled red laser diodes	720 nm - 820 nm	Optical efficiency	27 %
Gusakova et al. (2025)	Alexandrite laser based Q-switched	Xenon flash-lamps	729 nm	Slope efficiency	0.3 %

Tawy et al. (2023) proposed several cavity designs to enhance the output power of diode-pumped Alexandrite lasers; however, the influence of the structural materials used in the cavity framework was not examined. The cavity configurations were developed by varying the type and position of the mirrors. In particular, employing a four-mirror ring laser design, an optical efficiency of 27% was achieved. Nevertheless, this configuration was found to be unsuitable in terms of spatial requirements for low-loss cavities (< 0.1 %).

Gusakova et al. (2025) designed a KD*P Pockels cell driver to Q-switch the laser cavity and induce a sharp falling edge of the laser pulse with nanosecond precision. The driver was implemented as a high-voltage switching device, enabling the positronium–laser interaction time to be controlled on the nanosecond scale. In the employed laser system, a C-cut Alexandrite crystal rod, Cr (0.15 at. %):BeAl2O4, was used as the gain medium. The Alexandrite crystal was optically pumped by two xenon flash-lamps, each with a maximum discharge energy of 160 J. The achieved slope efficiency was 0.3 %, which represents the electrical-to-optical conversion efficiency (EtO-E) of the flash-lamp pumping process, rather than the overall system efficiency.

As observed in the aforementioned studies, the conversion efficiency of diode pumped lasers typically exceeds 1%, whereas flash-lamp pumped configurations exhibit the opposite trend due to intrinsic system limitations. This discrepancy is further influenced by additional parameters governing the laser system dynamics. In the present work, a flash-lamp pumped Alexandrite laser was employed, primarily because flash-lamps provide superior beam quality and enhanced harmonic generation efficiency compared with diode sources. In contrast, diode pumped lasers operate predominantly through optical-to-optical conversion pathways, where slope efficiency and optical-to-optical efficiency are the principal performance metrics. Flash-lamp pumped lasers, however, involve electrical-to-optical energy conversion (EtO−E). Hence, in this study, the evaluation focused on electrical-to-optical efficiency (η_{OCE}) rather than slope efficiency.

To the best of the authors' knowledge, and in contrast to prior reports, BK7 glass was utilized for the first time as the cavity skeleton material. The experimental results demonstrate that the integration of BK7 significantly enhanced both the optical efficiency and the overall system efficiency, highlighting the critical role of cavity skeleton material selection in efficiency scaling behavior.

5. Conclusion

This study has investigated the enhancement of optical conversion efficiency in a flash-lamp-pumped Alexandrite solid-state laser through structural modifications to the optical cavity. Unlike diode-pumped lasers, which operate via optical-to-optical conversion and typically demonstrate efficiencies above 1 %, flash-lamp–pumped systems are constrained by electrical to optical energy conversion pathways resulting in lower efficiencies. Nevertheless, flash-lamps remain advantageous due to their superior beam quality and harmonic generation capability, making them attractive for Alexandrite based laser systems.

To address the limitations of conventional designs, the cavity frame material is redesigned by replacing the fused silica (Quartz) structure with a borosilicate (BK7) framework while maintaining the original three-hole configuration. Experimental results demonstrated that the BK7 based cavity provided higher electrical to optical efficiency than quartz, achieving up to a 13 % improvement in overall system performance. These findings highlight that cavity skeleton material selection plays a critical role in scaling system efficiency, reducing energy consumption and extending operational lifetime.

In conclusion, the use of BK7 glass as an alternative to quartz in Alexandrite laser resonator design not only improves optical efficiency but also offers a cost-effective solution with comparable or superior optical characteristics. This material based optimization contributes a novel perspective to solid-state laser engineering, providing new insights for future development of high performance and energy efficient flash-lamp-pumped laser systems.

6. Limitations and Future Works

Thermal effects are an important consideration in high-energy laser systems. The laser device used in this study operates in a controlled laboratory environment with an ambient temperature maintained between $18-25^{\circ}C$ (optimum $22^{\circ}C$). Given the high thermal load generated during laser operation, ambient conditions are critical, as the system relies on air-assisted cooling to dissipate heat from the radiator through which the cooling water circulates.

The laser head is actively cooled using water maintained in the $60-65^{\circ}C$ range, and the system is designed to trigger a fault and cease operation if the cooling water temperature exceeds $70^{\circ}C$. Temperature regulation is performed with a precision of approximately $\pm 0.5^{\circ}C$. In the present work, the laser was operated under standard conditions using its original configuration, with the only modification being the replacement of the quartz element in the laser head with BK7 glass. While this modification may have slightly altered the thermal load of the system, no dedicated thermal monitoring was performed, as the operating temperature never exceeded the safety threshold and no thermal faults were observed.

For instance, after 1000 consecutive pulses, the cooling water temperature differed only marginally between configurations (e.g., $67.2^{\circ}C$ vs $68^{\circ}C$). Since the system remained within its nominal operating range in all cases, such minor thermal variations were considered negligible with respect to system performance. Although elevated temperatures can adversely affect flash-lamp lifetime, the small temperature differences observed in this study are not expected to introduce measurable effects in the experimental outcomes.

To further mitigate thermal bias, two laser heads with closely matched designs were fabricated and tested under identical operating conditions. In addition, the modified design was evaluated in a newer, higher-tier laser system, where it was operated for approximately one year, accumulating over 9.5 million pulses, with flash-lamp replacement occurring at intervals of approximately 1.8–2 million pulses. From an operational and user perspective, no significant or perceptible performance differences attributable to thermal effects were observed.

Future work may include real-time thermal profiling of the laser head and flash-lamp under extended operation to quantitatively assess subtle thermal differences introduced by cavity material variations. Such measurements would further strengthen the understanding of long-term thermal behavior and component aging in modified cavity designs.

Author Contributions

The percentages of the authors' contributions are presented below. All authors reviewed and approved the final version of the manuscript.

	R.T.	G.U.K.
C	50	50
D	50	50
S	30	70
DCP	70	30
DAI	70	30
L	50	50
W	40	60
CR	40	60
SR	40	60

C= concept, D= design, S= supervision, DCP= data collection and/or processing, DAI= data analysis and/or interpretation, L= literature search, W= writing, CR= critical review, SR= submission and revision.

Conflict of Interest

The authors declared that there is no conflict of interest.

Ethical Consideration

Ethics committee approval was not required for this study because of there was no study on animals or humans.

Acknowledgments

The authors acknowledge that the language and readability of this manuscript were improved through grammatical revision using AI-generated (ChatGPT-GPT-4o) text assistance.

References

Almabouada, F., Louhibi, D., Hamici, M., Hammoum, Y., & Haddouche, A. (2011). Power supply for xenon flash-lamp. *SIPP 2011*, 250–254.

Arieli, R. (2025). *The laser adventure: Chapter 6.2.3*. Weizmann Institute of Science. https://perg.phys.ksu.edu/vqm/laserweb/ch-6/F6s2t3p4.htm

Aslam, A., & Alster, T. S. (2014). Evolution of laser skin resurfacing: From scanning to fractional technology. *Dermatologic Surgery*, *40*(11), 1163–1172. https://doi.org/10.1097/01.DSS.0000452648.22012.a0

Azadgoli, B., & Baker, R. Y. (2016). Laser applications in surgery. *Annals of Translational Medicine*, *4*(23), 452. https://doi.org/10.21037/atm.2016.11.51

Bavi, E. P., Jouybari, S. N., & Mousavi, F. (2022). A rapid method for producing highly diffuse reflective white paint as the back surface reflector in dye-sensitized solar cell. *Optical Materials*, *131*(1), 112647. https://doi.org/10.1016/j.optmat.2022.112647

Bernstein, E., & Adrian, R. (2006). Tattoo and nevus of ota removal with Q-switched ruby laser: Case reports. *Cosmetic Dermatology*, *19*(6), 411–414. https://cdn.mdedge.com/files/s3fs-public/Document/September-2017/019060411.pdf

Bohacek, P. (2022). Peaceful use of lasers in space? Potential, risks, and norms for using lasers in space. *Space Policy*, *61*(1), 101489. https://doi.org/10.1016/j.spacepol.2022.101489

Candela Corporation. (2010). *GentleLase plus applications descriptions specifications Operator's Manual: (P/N 8501-00-1740, Revision A)*. Scanlan Group B.V. http://www.frankshospitalworkshop.com/equipment/documents/various_equipment/user_manuals/various/Candela%20GentleLase%20Dermatology%20Laser%20-%20User%20manual.pdf

Cheng, D. K. (2017). *Mühendislik elektromanyetiğinin temelleri* (2. Baskı). Palme Yayınevi.

Dharmadhikari, J. A., Dharmadhikari, A. K., Bhatnagar, A., Mallik, A., Singh, P. C., Dhaman, R. K., Chalapathi, K., & Mathur, D. (2011). Writing low-loss waveguides in borosilicate (BK7) glass with a low repetition-rate femtosecond laser. *Optics Communications*, *284*(2), 630–634. https://doi.org/10.1016/j.optcom.2010.09.055

Eichler, H. J., Eppich, B., Fischer, J., Güther, R., Gurzadyan, G. G., Hermerschmidt, A., Laubereau, A., Lopota, V. A., Mehl, O., Vidal, C. R., Weber, H., & Wende, B. (2005). *Laser physics and applications*. Subvolume A: Laser Fundamentals, Part 1. Weber, H., Herziger, G., & Poprawe, R. (Eds.). Springer. https://ehs.msu.edu/_assets/docs/laser/laser-fundamentals-pt1-springer-2005.pdf

Einstein, A. (1967). On the quantum theory of radiation. Haar, D. T. (Ed.). The Old Quantum Theory: A volume in the Commonwealth and International Library: Selected Readings in Physics, Part 2, 18(121), 167–183. Pergamon. https://doi.org/10.1016/C2013-0-02033-6

Flórez, P. B., Maz, H. H. A., Domínguez, J. A., Tost, A. J. E., & Páez, J. O. (2023). Histologic evaluation of effect of three wavelengths of diode laser on human gingival margins. *Journal of Lasers in Medical Sciences*, *14*(e61), 1–7. https://doi.org/10.34172/jlms.2023.61

Garrec, B. L. (2010). Laser-diode and flash lamp pumped solid-state lasers. *AIP Conference Proceedings*, 111–116. https://doi.org/10.1063/1.3426039

Gusakova, N., Camper, A., Caravita, R., Penasa, L., Glöggler, L. T., Wolz, T., Krumins, V., Gustafsson, F. P., Huck, S., Volponi, M., Rienacker, B., Khatri, G., Malamant, J., Mariazzi, S., Brusa, R. S., Cabaret, L., Comparat, D., & Doser, M. (2025). An alexandrite laser system for positronium laser cooling. *Optics & Laser Technology*, *182*(Part B), 112097. https://doi.org/10.1016/j.optlastec.2024.112097

Han, J., Zhang, F., Van Meerbeek, B., Vleugels, J., Braem, A., & Castagne, S. (2021). Laser surface texturing of zirconia-based ceramics for dental applications: A review. *Materials Science and Engineering: C*, *123*(1), 112034. https://doi.org/10.1016/j.msec.2021.112034

Hecht, J. (2018). *Understanding lasers: An entry-level guide* (4. Baskı). John Wiley & Sons. https://doi.org/10.1002/9781119310693

Jian, D., Hou, Z., Wang, C., Zhuo, M., Xiao, D., & Wu, X. (2021). Fabrication of fused silica microstructure based on the femtosecond laser. *AIP Advances*, *11*(9), 095218. https://doi.org/10.1063/5.0059443

Lawrence, J. (Ed.). (2018). *Advances in laser materials processing: Technology, research and applications* (2nd Edition). Woodhead Publishing. https://doi.org/10.1016/C2015-0-05718-5

Li, Z. Q, Wang, J. L., Wang, X. F., Allegre, O., Guo, W., Gao, W. Y., Xue, Y., & Li, L. (2020). Debris-free, zero taper cutting of BOROFLOAT 33 glass using a femtosecond Bessel laser beam. *Lasers in Engineering*, *46*(1), 383–393. https://www.oldcitypublishing.com/journals/lie-home/lie-issue-contents/lie-volume-46-number-5-6-2020/lie-46-5-6-p-383-393/

Luke, A. M., Mathew, S., Altawash, M. M., & Madan, B. M. (2019). Lasers: A review with their applications in oral medicine. *Journal of Lasers in Medical Sciences*, *10*(4), 324–329.

Mikhailov, M. M., Lapin, A. N., Yuryev, S. A., & Petrunina, N. V. (2021). On factors affecting the degradation of BaSO4 powders' optical properties under the action of the solar spectrum quanta. *Solid State Communications*, *326*(1), 114183. https://doi.org/10.1016/j.ssc.2020.114183

Parker, S. (2007). Introduction, history of lasers and laser light production. *British Dental Journal*, *202*(1), 21–31. https://doi.org/10.1038/bdj.2006.113

Poh, A. H., Jamaludin, M. F., Fadzallah, I. A., Ibrahim, N. M. J. N., Yusof, F., Adikan, F. R. M., & Moghavvemi, M. (2019). Diffuse reflectance spectroscopic analysis of barium sulfate as a reflection standard within 173-2500 nm: From pure to sintered form. *Journal of Near Infrared Spectroscopy*, *27*(6), 393–401. https://doi.org/10.1177/0967033519868241

Polyanskiy, M. N. (2024). Refractive index info database of optical constants. *Scientific Data*, *11*, 94. https://doi.org/10.1038/s41597-023-02898-2

Purohit, G. (2020). Overview of lasers. *Applied Innovative Research*, *2*(1), 193–203.

https://www.researchgate.net/publication/348574808_Overview_of_Lasers

Scheuer, S., Munk, A., Strotkamp, M., Haefner, C. L., Höffner, J., & Froh, J. (2024). Efficient intra-cavity frequency doubled, diode-pumped, Q switched alexandrite laser directly emitting in the UV. *Optics Express*, *32*(5), 7553–7563. https://doi.org/10.1364/OE.513731

Šulc, J., & Jelínková, H. (2013). 5- Solid-state lasers for medical applications. Helena Jelínková, (Ed.). In Woodhead Publishing Series in Electronic and Optical Materials, Lasers for Medical Applications, Woodhead Publishing, (pp. 127–176). https://doi.org/10.1533/9780857097545.2.127

Sun, X., Li, J., Hokansson, A., Whelan, D., & Clancy, M. (2009). Study of laser-induced damage to large core silica fiber by Nd:YAG and Alexandrite lasers. *Optical Fibers and Sensors for Medical Diagnostics and Treatment Applications IX*, *7173*OE. SPIE BiOS, 2009, San Jose, California, United States. https://doi.org/10.1117/12.807758

Svelto, O. (2010). *Principles of lasers* (5th Edition). Springer. https://doi.org/10.1007/978-1-4419-1302-9

Tawy, G., Minassian, A., & Damzen, M. J. (2023). Power-scaled CW Alexandrite lasers. *Applied Physics B*, *129*(3), 47. https://doi.org/10.1007/s00340-023-07989-x

Unland, S., Kalms, R., Wessels, P., Kracht, D., & Neumann, J. (2023). High performance cavity-dumped Q-switched Alexandrite laser CW diode pumped in double-pass configuration. *Optics Express*, *31*(2), 1112–1124. https://doi.org/10.1364/OE.478628

Watanabe, W., & Terai, S. (2020). Femtosecond laser integration of volume grating in BK7 glass refractive lens. *Optical Engineering*, *59*(4), 046109. https://doi.org/10.1117/1.OE.59.4.046109

Wu, J., Zhang, Y., Li, L. Q., Ren, Y., Lu, Q., Wang, L., & Chen, F. (2021). Raman spectra study on modifications of BK7 glass induced by 1030-nm and 515-nm femtosecond laser. *Results in Physics*, *21*(1), 103814. https://doi.org/10.1016/j.rinp.2021.103814

Xiao, H., & Damzen, M. J. (2024). High-efficiency 5-watt wavelength-tunable UV output from an Alexandrite laser. *Applied Physics B*, *130*(12), 209. https://doi.org/10.1007/s00340-024-08349-z

Yang, Y., Schwarz, S., Esen, C., & Hellmann, R. (2023). Influence of MHz bursts on the ablation efficiency of fused silica. *Journal of Laser Applications*, *35*(2), 022013. https://doi.org/10.2351/7.0001002

Yariv, A. (1991). *Optical electronics* (4th Edition). Philadelphia: Saunders College Publishing.

Yorulmaz, I., Beyatli, E., Kurt, A., Sennaroglu, A., & Demirbas, U. (2014). Efficient and low-threshold Alexandrite laser pumped by a single-mode diode. *Optical Materials Express*, *4*(4), 776–789. https://doi.org/10.1364/OME.4.000776

Song, Y., Wang, Z., Zhang, F., Bo, Y., Peng, Q. (2021). Continuous-wave Alexandrite laser pumped by 638 nm and 532 nm lasers. *Infrared and Laser Engineering, 50*(3), 1-7. https://www.sciengine.com/IRLA/doi/10.3788/IRLA20200217